JOURNAL OF Materials CHEMISTRY

Oriented growth of hydroxyapatite on (0001) textured titanium with functionalized self-assembled silane monolayer as template

Chuanbin Mao,* Hengde Li, Fuzhai Cui, Qinglin Feng, Hao Wang and Chunlai Ma

Department of Materials Science and Engineering, Tsinghua University, Beijing 100084, People's Republic of China

Received 18th February 1998, Accepted 19th August 1998

A highly (0001) textured hydroxyapatite [$Ca_{10}(PO_4)_6(OH)_2$, HA] coating on polycrystalline titanium plate is successfully synthesized by a biomimetic process mimicking biomineralization. To simulate the first stage of biomineralization, that is, supramolecular preorganization, a template surface with highly organized arrangement of carboxyl (−COOH) and alcoholic hydroxyl (−OH) groups is prepared through self-assembly of vinyltriethoxysilane [$(C_2H_5O)_3SiCH{=}CH_2$, VTS] on hydroxylated titanium with strong (0001) texture, followed by oxidation of the vinyl groups (−CH=CH_2) with dilute $KMnO_4$ solution into alcoholic hydroxyl and then into carboxyl groups. The functionalized substrate can induce oriented nucleation and growth of HA with (0001) planes parallel to the substrate surface from supersaturated HA solution through interfacial molecular recognition. The mechanisms of molecular recognition are also discussed.

1 Introduction

Biomineralization has been regarded as an excellent archetype for inorganic materials synthesis by materials chemists.[1] Four sequential stages are involved in the biomineralization including supramolecular preorganization, interfacial molecular recognition, vectorial regulation and cellular processing.[1] In recent years, with these four stages as archetypes, a new synthetic strategy, termed biomimetic synthesis or template synthesis, has been developed to synthesize a variety of inorganic materials such as nanoparticles,[2] thin films,[3] coatings,[3] porous materials[4] and materials with complex forms.[5] Currently, biomimetic synthesis of inorganic materials through a process mimicking biomineralization has been a very promising approach to prepare materials of low cost.[5]

To perform a successful biomimetic synthesis, it is most important to mimic the first stage of biomineralization (*i.e.*, supramolecular preorganization) where a highly organized reaction template is built through self-assembly of an organic matrix. For synthesis of films or coatings on inorganic substrates, a surface with organized functional groups is often prepared to act as reaction template through chemisorption and self-assembly of functional organic molecules on the substrates.[3,6,7] The functional molecules bond with the surface atoms which are usually coordinatively unsaturated. Therefore, the arrangement of the functional organic molecules is often determined by the surface lattice. For a single crystal substrate, the surface to be functionalized is always a single plane (*i.e.*, no grain boundaries and little variation in atomic arrangement). For a polycrystalline substrate, the arrangement of atoms usually differs significantly between two exposed crystal grains unless the substrate surface is highly textured with one plane preferably parallel to the surface, therefore the arrangement of chemisorbed and self-assembled functional molecules is usually not uniform and organized across the whole surface. Hence, the successful biomimetic growth of inorganic films or coatings is usually realized on self-assembled monolayer (SAM) covered single crystals.[6,7] However, practical films or coatings are usually on polycrystalline substrates, for example, the hydroxyapatite (HA) coating on titanium as biomedical bone implant. Therefore, it is necessary to find a way to obtain a highly organized functionalized surface on polycrystalline substrates.

We consider that one efficient way to increase the degree of organization of the arrangement of the functional molecules is to highly texture the substrate before functionalization through self-assembly, resulting in a large quantity of domains with nearly the same arrangement of surface atoms. Then a surface with a large quantity of domains with nearly the same arrangement of functional groups may be prepared after chemisorption and self-assembly of functional molecules. That is, an organized SAM can be fixed on a highly textured substrate through a self-assembly process.

In this paper, we hope to demonstrate the above consideration through biomimetic synthesis of an HA coating on polycrystalline titanium. The titanium is textured with (0001) preferably parallel to the surface through rolling deformation since the (0001) texture is a typical kind of rolling deformation induced texture for hexagonal metals.[8] The functionalized surface is prepared through initial hydroxylation with H_2O_2 and subsequent self-assembly of vinyltriethoxysilane (VTS), followed by oxidation of vinyl groups with dilute $KMnO_4$ solution into alcoholic hydroxyl groups and then into carboxyl groups. The principle of such a biomimetic process is illustrated in Fig. 1.

2 Experimental

2.1 Biomimetic synthesis

A supersaturated solution of HA ([Ca^{2+}] = 4mM) was prepared according to the procedure in ref. 9. A 2 mm thick titanium plate was prepared by rolling deformation to introduce the (0001) texture and was cut into small square pieces

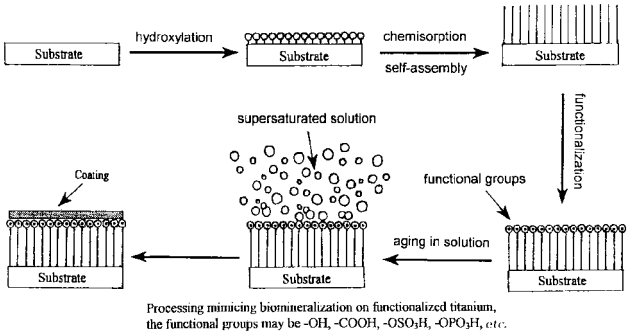

Fig. 1 Principle of biomimetic synthesis of HA coating on titanium through a process mimicking biomineralization.

(1 cm × 1 cm). The plates were metallographically polished with SiC emery paper to remove the oxide surface layer. The final polishing was performed with No. 800 paper and the final thickness of the polished plates was about 1 mm. The plates were ultrasonically washed in acetone for *ca.* 10 min and rinsed in deionized water for 1 min, and then placed in a 10% (by volume) solution of VTS in benzene for 2 weeks. After being rinsed in deionized water for several seconds, they were further aged in 5 mass% aqueous alkaline $KMnO_4$ solution first at 0 °C for one week and then in 5 mass% aqueous $KMnO_4$ solution containing sodium periodate ($NaIO_4$) at room temperature for one week. The resulting plates are denoted as VTS-Ti. One VTS-Ti plate was put into 50 ml HA solution and aged for up to 2 months. For comparison, a 1 cm × 1 cm × 2 mm control titanium plate with poor (0001) texture was prepared by a different rolling procedure,[8] and subjected to the subsequent experiment as above.

2.2 Characterization

The changes of pH during aging were measured *in situ* with a numeric acidity meter. The phase composition and orientation of the substrate and coating were determined by X-ray diffraction (XRD) on a Rigaku D/max RD diffractometer with a Cu target. To observe the morphologies of the coating by scanning electron microscopy (SEM), a knife was used to cut between the coating and the substrate, and then the coatings were fractured to expose a fresh fractured cross section, followed by coating with gold by ion beam sputtering. SEM images were observed by a Hitachi S-450 scanning electron microscope coupled with an energy dispersive X-ray analysis (EDAX) system. Functional groups were detected by X-ray photoelectron spectroscopy (XPS) on an ESCALAB 220i-XL system with Mg-Kα source.

3 Results

3.1 Coating formation

The XRD results in Fig. 2 indicate that the degree of (0001) texture of VTS-Ti is much higher than that of control VTS-Ti through the comparison of the relative intensity ratio between (0001) and (10$\bar{1}$1) diffraction peaks. Much different crystallization of calcium phosphate was observed by the naked eye upon aging both titanium plates in HA solutions. In HA solution containing VTS-Ti (VTS-Ti solution), crystallization only occurs on the surface of VTS-Ti to form a continuous white layer, indicating that heterogeneous nucleation and growth of calcium phosphates is favored on VTS-Ti. However, in the HA solution containing control VTS-Ti (control solution), crystallization occurs not only on the surface of control VTS-Ti to form several deposits of island-like white precipitates, and at the air/solution and solution/beaker interfaces to form island-like white precipitates, but also in the bulk solution to form floating white precipitates. In VTS-Ti solution, the white coating can be observed by the naked eye after about 2 days and grows thicker with aging for about one week. Crystallization elsewhere was not observed for up to 2 months. In the control solution, the island-like precipitates did not form a continuous layer for up to 2 months, which is consistent with the results of Hanawa and Ota.[10]

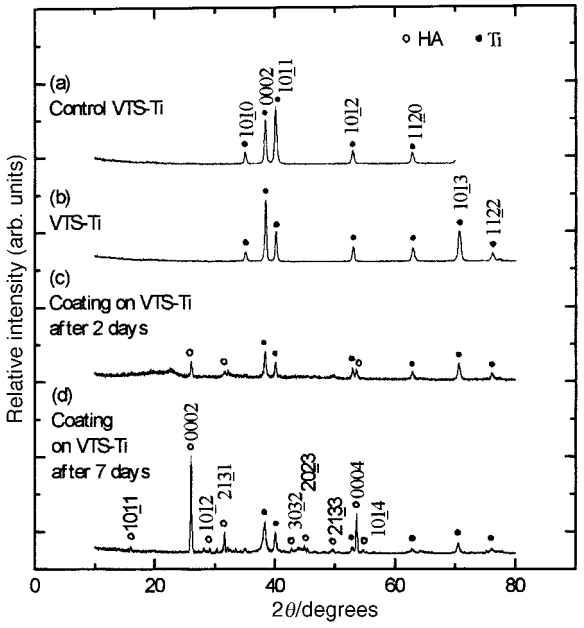

Fig. 2 XRD patterns of (a) control VTS-Ti; (b) VTS-Ti; (c) coating on VTS-Ti after 2 days and (d) coating on VTS-Ti after 7 days.

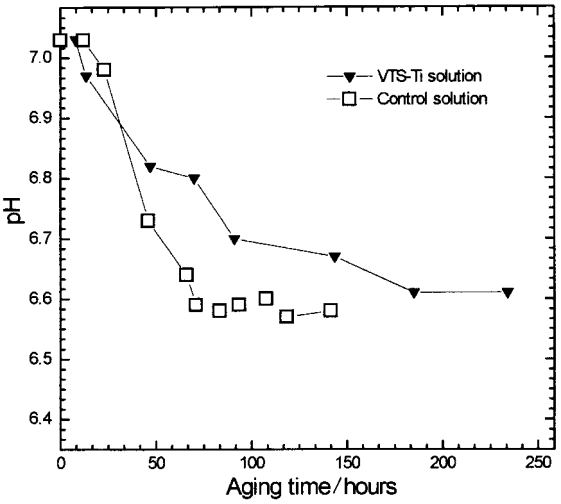

Fig. 3 Time dependences of pH in VTS-Ti solution and control solution.

Crystallization of HA can be written in terms of eqn. (1)

$$10Ca^{2+} + 6PO_4^{3-} + 2OH^- = Ca_{10}(PO_4)_6(OH)_2 \quad (1)$$

and reduction of pH can be an effective indicator of HA crystallization on titanium or elsewhere in the bulk solution. Fig. 3 depicts the time dependences of pH values of the VTS-Ti solution and control solution. The pH of the VTS-Ti solution decreases after an incubation period due to the crystallization on VTS-Ti and levels off at about 6.6 after about one week indicative of a typical nucleation and growth process. For the control solution, the pH begins to decrease a little later and then decreases more rapidly. It also levels off at about 6.6 after *ca.* 3 days.

3.2 Coating characterization

The XRD spectrum for VTS-Ti aged for 2 days as shown in Fig. 2(c) suggests that the HA crystals have nucleated and grown with (0001) preferably parallel to the substrate. After VTS-Ti has been aged for 7 days, *i.e.*, when the coating on VTS-Ti no longer grows as judged from a constant solution pH (Fig. 3) the coating is composed of highly (0001) textured HA as shown in Fig. 2(d). Since only several small deposits of island-like precipitates occur on the control VTS-Ti, they can not be characterized by XRD and thus SEM-EDAX is adopted. Fig. 4 shows the SEM morphologies of the fractured cross-sections of the coating on VTS-Ti at different stages. After being aged for 2 days [Fig. 4(a)], the coating on VTS-Ti is *ca.* 10 μm thick. Previous studies have shown that HA grains always tend to grow along the [0001] direction, which

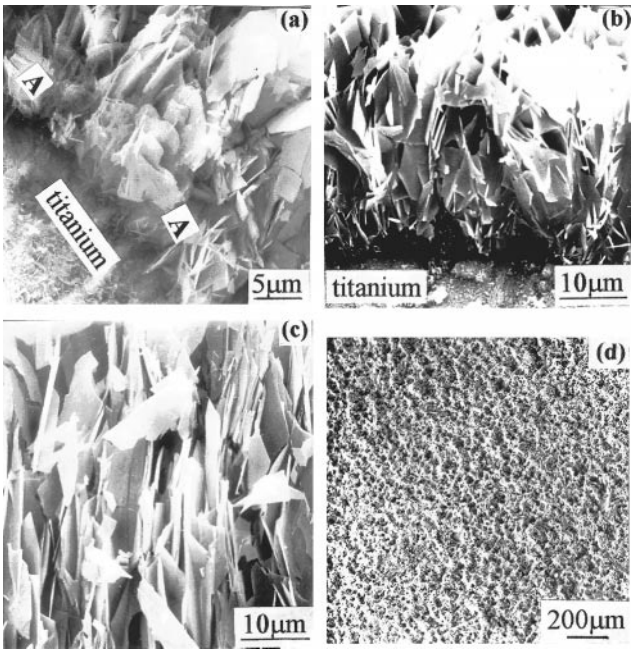

Fig. 4 SEM morphologies of the fractured cross sections of coatings on VTS-Ti, after 2 (a), 4 (b) and 7 days (c). A top-view SEM morphology of the coating on VTS-Ti after 7 days is shown in (d). Regions **A** in (a) denote the crystallization area that is not on SAM-$(110)_{TiO_2}$ domains. Note that the incident electron beam was tilted by 45° in (a), (b) and (c).

results in a plate habit, and the long axes of the plate-like grains are parallel to the crystallographic [0001] direction.[11] Thus, one can judge the type of preferred orientation by the fashion of the grain arrangements shown in the SEM images. From Fig. 4(a), one can observe that the HA crystals have been oriented with [0001] perpendicular to the substrate, consistent with the XRD result in Fig. 2(c). After 4 days [Fig. 4(b)], the coating is *ca.* 30 μm thick and the highly (0001) textured state is very obvious in the SEM figure. After 7 days [Fig. 4(c)], the coating is *ca.* 40 μm thick and consists of highly textured plate-like HA grains, consistent with the XRD result in Fig. 2(d). From the top-view SEM morphology of the coating on VTS-Ti [Fig. 4(d)], one can see that the coating is nearly uniform across the whole surface. The above results suggest that HA crystals nucleate on VTS-Ti with (0001) preferably parallel to the substrate and grow toward the solution, giving rise to a textured coating with the thickness equal to the length of one HA crystal along the [0001] direction. Fig. 5 shows the top-view SEM morphologies of the island-like precipitates on the control VTS-Ti after 7 days. This reveals that the precipitates consist of islands, which are significantly different from the coating on VTS-Ti as shown in Figs. 4(c) and (d). The islands are ball-like in shape and their size ranges between 50 and 150 μm. They are composed

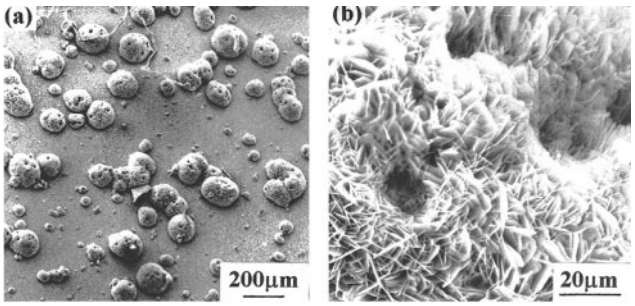

Fig. 5 Top-view SEM morphologies of island-like precipitates on control substrate after aging for one week: (a) whole morphology and (b) one island at higher magnification.

of plate-like HA grains which are *ca.* 10 μm wide. Since it is difficult to make a fractured cross-section of one island, the length of the HA grains can not be determined. However, analogous to the grains on VTS-Ti, the length of HA grains may be *ca.* 40 μm. Most of the ball-like islands are much thicker than the coating on VTS-Ti. This is because there are several HA grains along the normal of the substrate. From the SEM images in Fig. 5(b), the plate-like HA grains have grown toward the solution preferably with [0001] parallel to the normal of the substrate. These results demonstrate our considerations in section 1, that is, a functionalized surface on the textured substrate can be an effective template for biomimetic growth.

4 Discussion

4.1 Formation of an organized and hydroxylated surface

After the old oxide surface layer is removed through polishing, a fresh oxide layer will quickly form on the plate. Fig. 6 shows the XPS Ti 2p spectrum of a titanium surface before treatment with H_2O_2. Curve-fitting revealed that the spectrum can be resolved into two peaks centered at 463.89 and 458.27 eV, corresponding to Ti $2p_{1/2}$ and Ti $2p_{3/2}$ in TiO_2, respectively.[12,13] It is thus evident that the surface oxide layer of titanium is TiO_2. Many researchers also found that TiO_2 is the natural oxide layer on the titanium at room temperature.[13–15] Since the thermodynamically stable form of TiO_2 at low temperature is anatase (tetragonal, $a=0.3783$ nm, $c=0.951$ nm, JCPDS 4-477),[16] the surface oxide layer can be regarded as the anatase form.[17] Recently, Azoulay *et al.*[18] made a systematic investigation on the interactions of oxygen with polycrystalline titanium surfaces at a very low pressure of O_2. They found that the initial accumulation of oxygen follows an island formation model, resulting in a patch-like pattern of oxide surface layer containing different titanium valence states, and the oxide with better lattice match with underlying parent titanium structure will be favored to form first. Ti_2O (hexagonal, $a=0.29593$ nm, $c=0.4845$ nm, JCPDS 11-218) shows the best lattice match with titanium ($a=0.2950$ nm, $c=0.4686$ nm, JCPDS 5-682) among all the titanium oxides and can be directly transformed from titanium through the ordering of the dissolved oxygen atoms (*cf.* notes on JCPDS 11-218). Electron microscopy also revealed that Ti_2O can grow out of titanium through coherent transformation.[19] In addition, Ti_2O has the lowest content of oxygen among all the titanium oxides.[20] Consequently, the fresh surface oxide layer, which is too thin to be detected by XRD, may be formed from Ti directly to TiO_2, or through intermediate oxides with low oxygen content, *i.e.*, low chemical valence of titanium, such as Ti_2O, and finally to TiO_2. The intermediate Ti_2O will be also (0001) textured due to coherent transformation from (0001) textured titanium. Since there is a good lattice matching

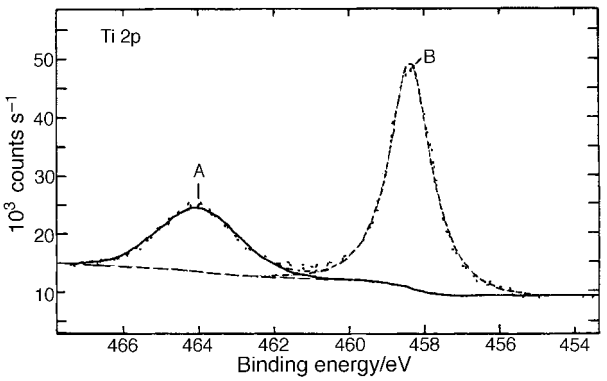

Fig. 6 Curve-fitting of the Ti 2p XPS spectrum for titanium before H_2O_2-treatment.

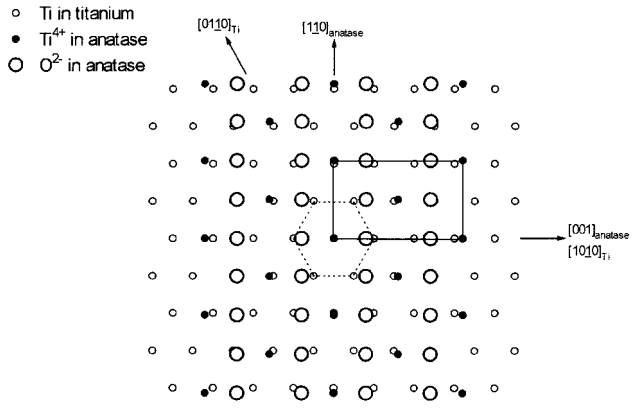

Fig. 7 Schematic illustration of the lattice match between $(0001)_{Ti}$ and $(110)_{anatase}$. The dashed and bold line frames show the outlines of the unit cells of Ti along [0001] and TiO_2 along [110], respectively.

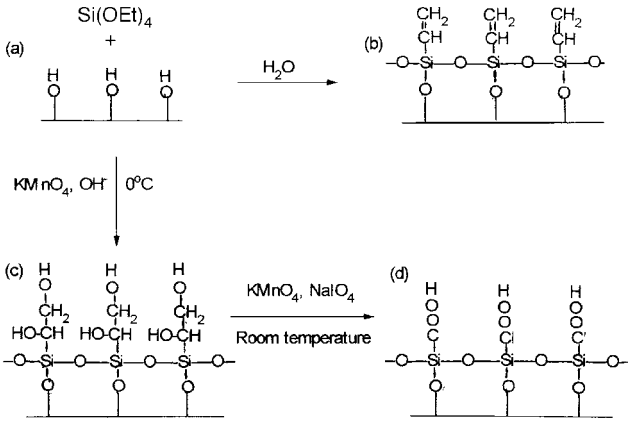

Fig. 8 Schematic illustration of formation and functionalization of a self-assembled silane monolayer.

between $(0001)_{Ti}$ or $(0001)_{Ti_2O}$ and $(110)_{anatase}$ (for structure of anatase see ref. 16) as illustrated in Fig. 7, the transformed TiO_2 will be (110) textured due to the (0001) texture of underlying titanium and may be why the texture of substrate before SAM-functionalization plays an important role in biomimetic mineralization of HA. It should be stated that the process of surface oxidation on titanium in air has scarcely been studied perhaps because the oxidation from Ti to TiO_2 is very quick and TiO_2 is always the main detected oxide.[13–15]

During subsequent aging in H_2O_2 solution, a surface interaction will occur between the fresh oxide layer formed on the titanium and H_2O_2 to form active hydroxyl groups.[21,22] The peroxide ion (O_2^{2-}) can be regarded as an active state of O_2. Its electron configuration is σls^2, $\sigma^* ls^2$, $\sigma 2s^2$, $\sigma^* 2s^2$, $\sigma 2p_x^2$, $\pi 2p_y^2$, $\pi 2p_z^2$, $\pi^* 2p_y^2$, $\pi^* 2p_z^2$, $\sigma^* 2p_x^0$ where σ and π refer to bond-forming orbitals, and σ^* and π^* to antibonding orbitals, respectively and there is an empty $\sigma^* 2p_x$ orbital in O_2^{2-}.[21,22] The coordinatively unsaturated surface (c.u.s.) Ti^{4+} ions have unbonded valence electrons and will interact with O_2^{2-} in H_2O_2. The coordinatively saturated bulk Ti^{4+} ions show an outermost electron configuration of $3d^0 4s^0$. Some c.u.s. titanium sites may occur as Ti^{3+} ($3d^1 4s^0$).[23,24] During the surface reaction, 3d electrons will be favored to enter empty $\sigma^* 2p_x$ orbitals, resulting in cleavage of the O–O bond in O_2^{2-} and thereby the formation of hydroxyl groups (–OH).[21,22] The fresh –OH will be thermodynamically favored to be chemisorbed on the surface oxide layer through bonding with c.u.s. Ti^{4+} ions.[17,25] In addition, chemisorbed hydroxyl groups can also be formed through dissociation of H_2O on titanium. However, the concentration of such chemisorbed hydroxyl groups is very low because the major part of H_2O is physisorbed.[17,25] Hence, a highly hydroxylated surface will be realized after H_2O_2 treatment. The chemisorbed hydroxyl groups on the c.u.s. Ti^{4+} ions of the fresh oxide layer can be denoted as Ti–OH. Moreover, the texturing of the substrate before chemisorption of hydroxyl groups makes a majority of TiO_2 crystals with (110) planes exposed, that is, a majority of domains with same c.u.s. Ti^{4+} arrangement on surface and thus a majority of domains with the same arrangement of Ti–OH. Consequently, the OH groups on the textured substrate are more organized than a nontextured substrate, and may be more suitable to act as a template for biomimetic growth of coatings after further functionalization.

4.2 Formation of a self-assembled monolayer (SAM)

According to known organic processes,[26] vinyl groups will be oxidized by dilute $KMnO_4$ solution first to give alcoholic hydroxyl groups at low temperature and then into carboxyl groups at room temperature and the formation of VTS-SAM and further functionalization of SAM is illustrated in Fig. 8.[27]

To demonstrate the formation of functionalized SAM, VTS-Ti was subjected to XPS characterizations. Fig. 9 shows the O 1s XPS spectrum of VTS-Ti. Curve-fitting revealed three peaks with binding energies of 533.04, 531.32 and 529.65 eV, corresponding to O 1s electrons in –O–Si(O)–O–Si(O)–O–(like SiO_2), –COOH and –OH, and surface oxide lattice, respectively.[12] It is worthwhile to point out that due to adsorption of some other phases containing oxygen such as H_2O and $KMnO_4$, their contribution in O 1s photoemission peaks may be overlapped and cannot be resolved from the above species. For example, the O 1s binding energy in $KMnO_4$ is very similar to that in –COOH.[12] Therefore, the C 1s XPS spectrum (Fig. 10) may be more suitable to characterize the functionalized SAM. Curve-fitting showed three peaks with binding energies of 288.24, 286.02 and 284.63 eV, which correspond to carbon in –COOH, $-CH(OH)CH_2OH$, $-CH{=}CH_2$

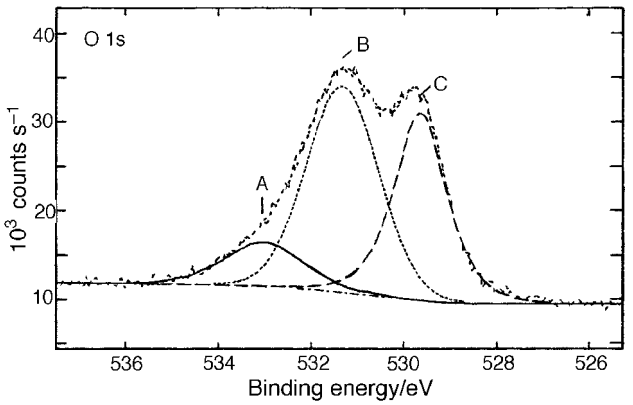

Fig. 9 Curve-fitting of the O 1s XPS spectrum for VTS-Ti.

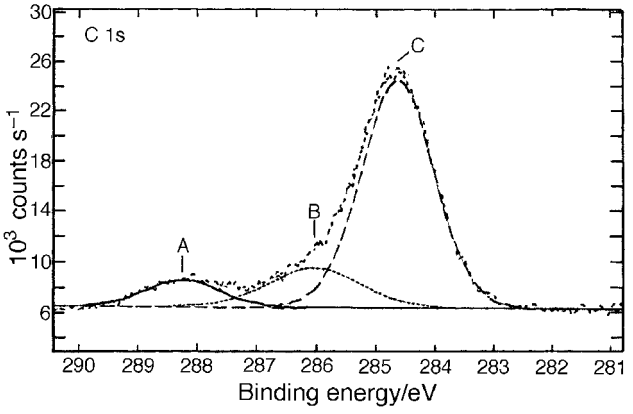

Fig. 10 Curve-fitting of the C 1s XPS spectrum for VTS-Ti.

and contaminated carbon inherent to the XPS spectrometer, respectively.[12,28] These results suggest that the oxidation of $-CH=CH_2$ into $-CH(OH)CH_2OH$ and further into $-COOH$ is not complete, which is characteristic for this organic reaction. Therefore, the SAM on VTS-Ti is a mixture of OH-terminated and COOH-terminated silane moleculars fixed on the titanium plate, *i.e.*, a mixture of states as shown in Fig. 8(b)–(d). Since we are dealing with a self-assembly process and the hydroxylated surface on highly (0001) textured titanium is highly organized, the mixture may be uniform, *i.e.*, the arrangement of $-CH=CH_2$, OH and COOH groups in the functionalized SAM on highly textured titanium is highly organized. Among these groups, OH and COOH can induce biomimetic mineralization[6,7] and may be the reason why control VTS-Ti can not induce coating formation; this will be discussed later.

4.3 Mechanism of oriented coating formation

In biomineralization, oriented nucleation and growth result from the mediation by preorganized supramolecules through interfacial molecular recognition including the complementarities of lattice geometry, electrostatic potential, polarity, stereochemistry, space symmetry and topography.[1] Similarly, in this biomimetic synthesis, the oriented nucleation and growth of HA originate from the regulation by OH- and COOH-functionalized SAM fixed on textured titanium through interfacial molecular recognition.

The interfacial molecular recognition involves at least four aspects: (1) Crystal lattice matching. The arrangement of OH and COOH groups in SAM fixed on the (110) oriented TiO_2 layer along $[001]_{anatase}$ shows excellent one-dimensional (1-D) coherent matching with the (0001) plane of HA along $[01\bar{1}0]_{HA}$ as illustrated in Fig. 11.[29] (2) Hydrogen bonding interaction. OH and COOH on SAM can form hydrogen bonds not only with OPO_3^{3-} on (0001) planes of HA, *i.e.*, $OH\cdots OPO_3$ and $COOH\cdots OPO_3$,[29,30] but also with OH^- on the (0001) planes of HA, *i.e.*, $OH\cdots O{-}H$ and $COOH\cdots O{-}H$, respectively. (3) Electrostatic potential interaction. The negatively charged COO^- on SAM can attract the positively charged Ca^{2+} in HA solution to substrate surface. (4) Stereochemistry match. The directions of the valence bonds of OH and OH in COOH tend to be parallel to that of O–H on (0001) planes of HA (parallel to the *c*-axis of HA).[29]

The recognition elements (1) and (4) explain why (0001) textured HA is favored to form. Now one can understand why VTS-Ti can induce formation of (0001) textured HA coating while control VTS-Ti can only induce formation of island-like precipitates, and moreover, both the coating on VTS-Ti and the island-like precipitates on the control substrate exhibit order on a length scale larger than the expected size of SAM-$(110)_{TiO_2}$ domains as shown in Fig. 4 and 5. This can be explained by the formation process of HA on the substrate as illustrated in Fig. 12. On VTS-Ti, many domains are exposed with (110) planes of TiO_2 and functionalized with OH or COOH groups and thus there will be many domains in which all the above molecular recognition processes are active and induce oriented nucleation and growth of HA with (0001) planes parallel to VTS-Ti. Therefore, HA crystals nucleate preferably on many SAM-$(110)_{TiO_2}$ domains with (0001) preferably parallel to the substrate on such domains [Fig. 12(a)]. As these crystals are growing toward solution along the [0001] direction, HA crystals will also begin to nucleate and grow on other SAM domains in the nearby pores between SAM-$(110)_{TiO_2}$ domains close to the growing crystals in a side-by-side fashion, through the above recognition processes except lattice matching between SAM and nuclei and 2-D lattice matching along substrate normal to the growing HA crystals and the new nuclei[31] [Fig. 12(b) and (c)]. The crystals grown according to this fashion are labelled **A** in Fig. 4(a).

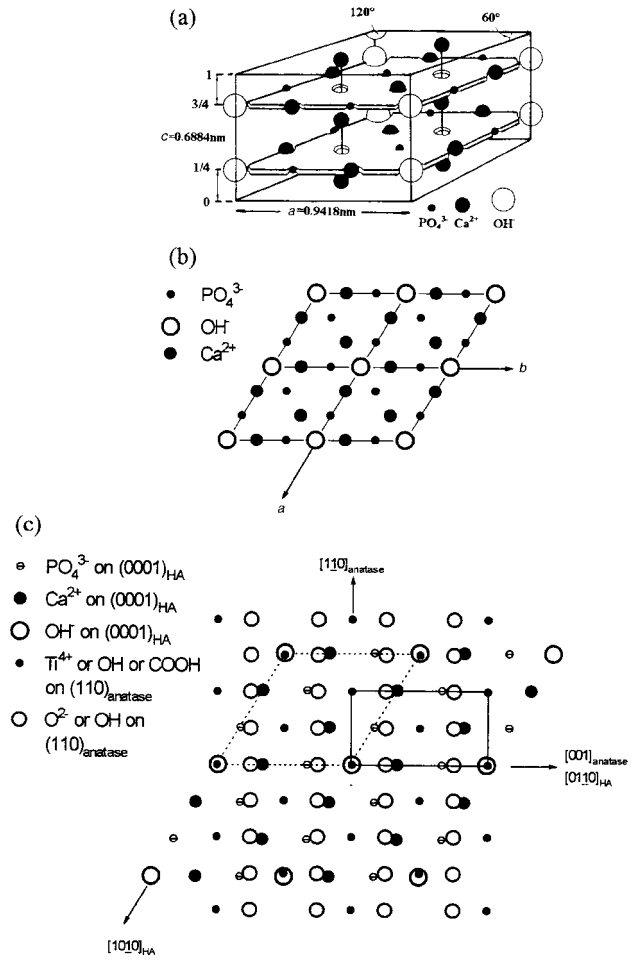

Fig. 11 Schematic illustration of the one-dimensional lattice match relation between (0001) planes of HA and SAM treated TiO_2. (a) Idealized crystal structure of HA[30] (note that the atomic arrangement of PO_4 and OH is not resolved for clarity), (b) (0001) plane of HA at $z=3/4$ and (c) lattice overlapping between the functionalized (110) plane of TiO_2 and (0001) plane of HA. The dashed and bold line frames show the outlines of the unit cells of HA along [0001] and TiO_2 along [110], respectively.

Thus finally a continuous textured coating can be formed on VTS-Ti [Fig. 12(d)]. However, on control VTS-Ti, few isolated domains are exposed with (110) planes of TiO_2, and then the effective molecular recognition, especially the 1-D lattice matching, can only occur on such few isolated domains. Consequently, for control VTS-Ti, after HA crystals nucleate and grow on these few SAM-$(110)_{TiO_2}$ domains as the case on VTS-Ti [Fig. 12(a′) and (b′)], the degree of supersaturation is relatively higher for HA to nucleate in head-to-head fashion, through a 2-D lattice match between (0001) planes of the new HA nuclei and the underlying HA crystals[31] [Fig. 12(b′) and (c′)] and also in other places such as the beaker/solution and air/solution interface. The distance between two SAM-$(110)_{TiO_2}$ domains is much longer for the control substrate than for VTS-Ti. For control VTS-Ti, before the crystallization can cover the exposed area between SAM-$(110)_{TiO_2}$ domains, the solution has been saturated. Therefore, there will be exposed areas where no HA crystallizes and island-like precipitates exist on the substrate [Fig. 12(d′)]. One can thereby understand why the height of islands on control substrate is much larger than that of the coating on VTS-Ti, and both the coating and the island-like precipitates show order on a length scale larger than the expected size of SAM-$(110)_{TiO_2}$ domains. It is possible that the final coating on VTS-Ti will tend to be uniform as shown in Fig. 4 because there will be a larger driving force for growth for smaller

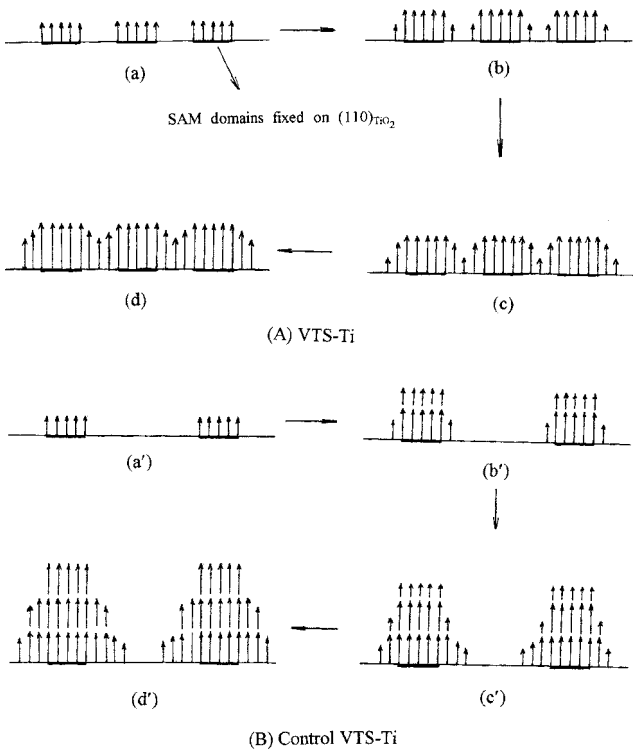

Fig. 12 Schematic illustration of the biomimetic mineralization process on (A) VTS-Ti and (B) control VTS-Ti. Note that the thicker and thinner lines correspond to the SAM domains fixed on $(110)_{TiO_2}$ and those on TiO_2 crystal surfaces except (110).

crystals (*i.e.*, HA crystals which nucleate later on SAM domains fixed on TiO_2 surfaces except (110)]. It seems that the geometry matching between the arrangement of functional groups and 1-D or 2-D crystal lattice of inorganic nuclei plays an important role in biomimetic mineralization. Further investigation of this point is now under way in our laboratory.

Another interesting result to be explained is the different time dependences of the pH values between VTS-Ti solution and control VTS-Ti solution. From reaction (1), it can be deduced that the more rapidly the HA crystals nucleate and grow, the more quickly the solution pH decreases. Therefore, the different time dependences of pH values reflect the different rates of HA crystallization. The pH-time curves in Fig. 3 can be resolved into three stages. The initial stage is the incubation period during which the pH value remains unchanged and no HA crystals are formed. The subsequent stage is the nucleation and growth period during which the pH decreases because OH^- ions are constantly incorporated into HA structure to make HA nucleate and grow together with PO_4^{3-} and Ca^{2+} ions. At this stage, HA crystals begin to nucleate and further grow into plate-like grains. The last stage is an equilibrium period when the pH value no longer changes because the solution has reached a saturated state. Such patterns are characteristic for crystallization which undergoes changes from the incubation period through nucleation and growth period to saturation. The incubation period for VTS-Ti solution (0–8 h) is shorter than that for control solution (0–12 h), whereas the nucleation and growth period for the former (8–180 h) is longer than that for the latter (12–70 h). During the incubation period, the ionic species (PO_4^{3-}, OH^-, Ca^{2+}) are bonded to the functionalized surface through molecular recognition, which will favor the subsequent nucleation and growth of HA, although HA crystals do not crystallize at this time. Because there are many more SAM-$(110)_{TiO_2}$ domains as reaction template for the above recognitions on VTS-Ti than on the control substrate, the nucleation and growth of HA will begin earlier on VTS-Ti than on control VTS-Ti, and the crystallization always occurs on VTS-Ti before elsewhere in the VTS-Ti solution while relatively few crystals crystallize on control VTS-Ti before crystallizing elsewhere in the control solution. Thus the pH decreases at a earlier stage in the VTS-Ti solution than in the control solution, *i.e.*, the incubation period is shorter in the VTS-Ti solution than in the control solution. After the incubation period, the crystallization on VTS-Ti is controlled by the reaction template through the above recognition in VTS-Ti solution. However, in the control solution, crystallization occurs elsewhere such as at the air/solution and beaker/solution interface besides the control substrate due to the existence of a much smaller area of the effective reaction template. Thus the pH value decreases more rapidly and levels off more quickly in the control solution than in the VTS-Ti solution, *i.e.*, the nucleation and growth period is longer in the VTS-Ti solution than in the control one.

4.4 Importance of texturing HA coatings

So far, there have been no reports concerning the successful synthesis of highly (0001) oriented HA coatings on titanium or other substrates by biomimetic or other processes.[3,32–36] In natural bone, HA is highly oriented with (0001) perpendicular to the collagen fibrils.[37] Therefore, as a bone implant material, it may be necessary for HA coating to be (0001) oriented to help growth of collagen fibrils in surrounding bone tissue into the implant to enhance biointegration.[35]

5 Conclusion

A highly oriented HA coating is successfully prepared by a biomimetic process on a textured titanium substrate. The oriented growth of HA results from the mediation by a functionalized self-assembled monolayer with organized arrangement of OH and COOH groups fixed on the textured titanium plate through interfacial molecular recognition such as crystal lattice matching, hydrogen bonding interaction, electrostatic potential interaction and stereochemistry match.

Acknowledgements

This project was granted financial support from China Postdoctoral Science Foundation.

References

1 S. Mann, *J. Mater. Chem.*, 1995, **5**, 935 and references therein.
2 F. J. Fendler and F. C. Meldrum, *Adv. Mater.*, 1995, **7**, 607.
3 B. C. Bunker, P. C. Rieke, B. J. Tarasevich, A. H. Campbell, G. E. Fryxell, G. L. Graft, L. Song, J. Liu, J. W. Virden and G. L. McLay, *Science*, 1994, **264**, 48.
4 Q. Huo, H. I. Margolese and G. D. Stucky, *Chem. Mater.*, 1996, **8**, 1147.
5 S. Mann and G. A. Ozin, *Nature*, 1996, **382**, 313.
6 H. Shin, R. J. Collins, M. R. De Guire, A. H. Heuer and C. N. Sukenik, *J. Mater. Res.*, 1995, **10**, 692.
7 H. Shin, R. J. Collins, M. R. De Guire, A. H. Heuer and C. N. Sukenik, *J. Mater. Res.*, 1995, **10**, 699.
8 J. H. Keeler, W. R. Hibbard and B. F. Decker, *Trans. AIME*, 1953, **197**, 932.
9 H. B. Lu, C. L. Ma, H. Cui, L. F. Zhou, R. Z. Wang and F. Z. Cui, *J. Cryst. Growth*, 1995, **155**, 120.
10 T. Hanawa and M. Ota, *Appl. Surf. Sci.*, 1992, **55**, 269.
11 M. Kukura, L. C. Bell, A. M. Posner and J. P. Quirk, *J. Phys. Chem.*, 1972, **76**, 900.
12 C. D. Wagner, W. M. Riggs, L. E. Davies, J. F. Moulder and G. E. Muilenberg, *Handbook of X-ray photoelectron spectroscopy*, Perkin-Elmer Corporation, Eden Prairie, MN, 1979, pp. 58–70.
13 C. N. Sayer and N. R. Armstrong, *Surf. Sci.*, 1978, **77**, 301.
14 E. Bertel, R. Stockbauer and T. E. Mady, *Surf. Sci.*, 1984, **141**, 355.
15 D. E. Eastman, *Solid State Commun.*, 1972, **10**, 933.

16 K. I. Hadjiivanov and D. G. Klissurski, *Chem. Soc. Rev.*, 1996, **25**, 61.
17 T. Hanawa, M. Kon, H. Ukai, K. Murakami, Y. Miyamoto and K. Asaska, *J. Biomed. Mater. Res.*, 1997, **34**, 273.
18 A. Azoulay, N. Shamir, E. Fromm and M. H. Mintz, *Surf. Sci.*, 1997, **370**, 1.
19 K. Huelse and K. H. Kramer, in *Titanium Science and Technology*, ed. G. Luetjering, U. Zwicker and W. Bunk, Deutsche Gesellschaft fuer Metallkunde e. V., Germany, 1984, vol. 2, p. 1072.
20 P. G. Wahlbeck and P. W. Gilles, *J. Am. Ceram. Soc.*, 1966, **49**, 180.
21 J. Weis, *Adv. Catal.*, 1952, **4**, 343.
22 J. C. Bailar, *Comprehensive Inorganic Chemistry*, Pergamon Press, 1973, vol. 2, p. 685.
23 K. Hadjiivanov, A. Davydev and D. Klissurski, *Kinet. Katal.*, 1988, **29**, 161.
24 K. Hadjiivanov, O. Saur, J. Lavnotte and J. C. Lavalley, *Z. Phys. Chem.* (*Munich*), 1994, **187**, 1281.
25 C. Morterra, *J. Chem. Soc.*, *Faraday Trans.*, 1988, **84**, 1617.
26 R. T. Morrison and R. N. Boyd, *Organic Chemistry*, Prentice Hall, New Jersey, 1992, 6th edn., pp. 357–360.
27 T. B. McPherson, H. S. Shim and K. Park, *J. Biomed. Mater. Res.*, 1997, **38**, 289.
28 G. Beamson and D. Briggs, *High resolution XPS of organic polymers*, *the Scienta ESCA300 database*, John Wiley & Sons, New York, 1992, pp. 66, 116.
29 T. Hanazawa, *Inorganic Phosphate Materials*, Elsevier, Amsterdam, 1989, pp. 24–29, 91–92.
30 P. F. Gonzalez-Diaz and M. Santos, *J. Solid State Chem.*, 1997, **22**, 193.
31 P. G. Koutsoukos and G. H. Nancollas, *J. Cryst. Growth*, 1981, **53**, 10.
32 C. Ohtsuki, H. Iida, S. Hayakawa and A. Osaka, *J. Biomed. Mater. Res.*, 1997, **35**, 39.
33 S. Li, Q. Liu, J. De Wijn, K. De Groot and B. L. Zhou, *J. Mater. Sci. Lett.*, 1996, **15**, 1882.
34 T. KoKubo, E. Miyaji, H. M. Kim and T. Nakamura, *J. Am. Ceram. Soc.*, 1996, **79**, 1127.
35 K. A. Khor, P. Cheang and Y. Wang, *J. Miner. Met. Mater. S*, 1997, **2**, 51.
36 C. Ohsuki, H. Iida, S. Hayakawa and A. Osaka, *J. Miomed. Mater. Res.*, 1997, **35**, 39.
37 A. Veis, *The Chemistry and Biology of Mineralized Connective Tissues*, Elsevier, Amsterdam, 1981, p. 617.

Paper 8/01384E